Application of CT Acquisition Parameters as Features in Computer-Aided Detection for CT Colonography

Janne J. Näppi[1], Don Rockey[2], Daniele Regge[3], and Hiroyuki Yoshida[1]

[1] 3D Imaging Research, Department of Radiology,
Massachusetts General Hospital and Harvard Medical School,
25 New Chardon St., Suite 400C, Boston, Massachusetts 02114, USA
jnappi@partners.org, yoshida.hiro@mgh.harvard.edu
[2] University of Texas Southwestern Medical School,
5323 Harry Hines Blvd, Dallas, Texas 75390-9151, USA
[3] Institute for Cancer Research and Treatment,
Candiolo Str. Prov. 142, IT-10060, Turin, Italy

Abstract. Studies have indicated that the acquisition parameters of computed tomography (CT) scans can have significant effect on the accuracy of computer-aided detection (CAD) in CT colonography. We investigated whether these parameters can be used as external features with conventional image-based features to improve CAD performance. A CAD scheme was trained with the CT colonography data of 886 patients, and it was tested with an independent set of 705 CT colonography cases. The results indicate that some CT acquisition parameters can be used successfully as features of the detected lesion candidates for improving the detection accuracy of CAD for flat lesions and carcinomas.

Keywords: Computed tomographic colonography, computer-aided detection, CT acquisition, polyp detection, virtual colonoscopy.

1 Introduction

Some of the acquisition parameters of computed tomography (CT) can have a significant effect on the detection accuracy of computer-aided detection (CAD) in CT colonography (CTC). Therefore, studies have been performed to determine the effect and optimal value of CT acquisition parameters for CAD in CTC. In two studies, the slice thickness of CTC images was observed to limit the size of the smallest polyp that is detectable by CAD [10,4]. In one study, CAD was applied to low-dose CTC by use of a 13 mAs/rotation, collimation of 1.5 mm, slice thickness of 3.0 mm, reconstruction interval of 1.5 mm, and table speed of 30 mm per rotation [3].

In practice, imaging devices are optimized for the purposes of visualization by radiologists rather than for the application of CAD. Therefore, it is likely that practical CAD systems will need to be able to adapt automatically to a wide variety of input data and parameter settings from multiple sources.

H. Yoshida, D. Hawkes, M.W. Vannier (Eds.): Abdominal Imaging 2012, LNCS 7601, pp. 69–77, 2012.

In a conventional application of CAD in CTC, the detected regions of lesion candidates are characterized in terms of shape-based and texture-based features. The features are collected into feature vectors that are analyzed by a classifier to determine the likelihood that a lesion candidate represents a true lesion. The detections with highest likelihood of being a lesion will represent the output of the CAD scheme.

In this study, we considered the application of CT acquisition parameters as additional external features of the lesion candidates. Because CT acquisition parameters affect the visual appearance of CTC images (Fig. 1), and because some of them are known to affect CAD performance anyway, we hypothesized that their use as additional features could improve the discrimination performance of the classifier used by a CAD scheme. By reflecting meaningful adjunct information about image contrast, volumetric isotropy, or smoothness of the reconstructed CTC image data, the CT acquisition parameters might be able to improve the efficacy of conventional image-based shape and texture features.

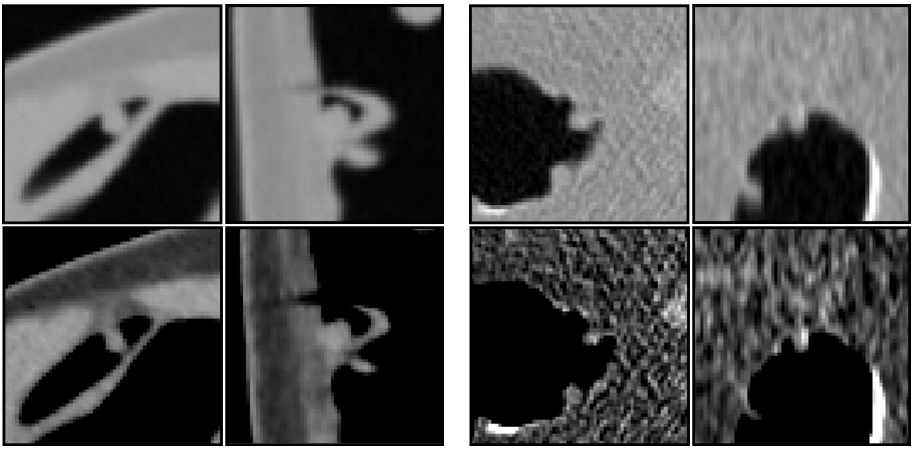

Fig. 1. Axial (left columns) and sagittal (right columns) CTC images of 7-mm polyps with wide (top rows) and narrow (bottom rows) display window settings. (a) Application of a soft reconstruction kernel, slice thickness of 1.0 mm, reconstruction interval of 0.8 mm, and tube current of 28 mA with 140 kVp. (b) Application of a soft reconstruction kernel, slice thickness of 2.5 mm, reconstruction interval of 1.25 mm, and tube current of 50 mA with 120 kVp.

The CT acquisition parameters that were used as external features in this study are described in Section 2.2. We considered only parameters that can be found in the file header of Digital Imaging and Communications in Medicine (DICOM) files. Furthermore, we considered only parameters that are likely to be associated with visually perceived image characteristics. For evaluation, each

external parameter was combined, one at a time, with a set of 6 conventional image-based shape and texture features that we have identified previously as the most effective and consistent features in polyp detection [7].

To provide a variety of examples of different CTC image acquisitions, and to avoid overfitting to a specific patient population or institution, we used a large number of CTC cases from multiple institutions. The evaluation was based on independent training and testing regimens. Statistical analysis was performed to assess the effect of the external features on the detection accuracy of CAD.

2 Methods

2.1 CAD Scheme

The fully automated CAD scheme that was used in this study processes an input CTC case in a number of steps. First, the CTC images are subjected to a pseudo-enhancement correction for minimizing tagging artifacts [8], and the volumetric data are interpolated to isotropic resolution [11]. Next, a thick region encompassing the colonic mucosa is extracted from input CTC data by use of a lumen-tracking method [7]. The locations of lesion candidates are determined by thresholding of lesion-like values of volumetric shape features of the extracted region [11]. The complete regions of detected lesion candidates are extracted by use of conditional morphological dilation [6]. Several shape and texture features are calculated for the regions of lesion candidates [5]. Finally, false-positive (FP) detections are reduced by use of a statistical classifier that determines the output of the CAD scheme [12].

Previously, we identified 6 shape and texture features that have emerged as consistently effective discriminative features over a wide variety of CTC populations [7]. In the following, we will denote this basic set of features as F6. For evaluation, each CT acquisition parameter (see Section 2.2) was combined with F6, one at a time, to yield sets of 7 features for the training and testing of the CAD scheme.

2.2 CT Acquisition Parameter Features

We considered the application of the following CT acquisition parameters as external features of lesion candidates:

- Slice thickness (ST). In a multi-detector array scanner, the ST is determined by binning of the different numbers of detector subunits together and by physically moving the collimator to the outer edges of the slices of a detector [1]. The image noise decreases when the slice thickness is increased.
- Reconstruction interval (RI). The RI defines the spacing of the reconstructed images. If the RI is too wide, small lesions that are located at the boundary between two slices could be missed due to partial-volume effects [9].
- Tube current (TC). A high TC reduces image noise, but it also increases radiation dose to the patient.

- In-plane image resolution (RS). The RS is the physical dimension of a pixel in a reconstructed CTC image.
- Focal spot (FS). The FS is the area on the anode of an x-ray tube that is struck by electrons and from which the resulting x-rays are emitted. An increment of focal spot size reduces the ability to define small structures.
- Exposure time (ET). The ET is the time during which the patient is exposed to radiation. A long scan time may cause in breathing artifacts.
- Reconstruction kernel (K). The K that is convoluted with the image data determines the relationship between spatial resolution and image noise.
- Slice ratio (SR). The SR is a unitless feature that we derived from DICOM header information to characterize the isotropy of the reconstructed volumetric CTC data. It is calculated as SR = RS/ST. A small value of SR indicates that the volumetric image data may be suffering from geometric distortions, whereas a large value indicates that the physical voxels have nearly isotropic resolution, thereby minimizing distortions of image structures.

Most of these parameters have numerical values. However, the value of the reconstruction kernel (K) is highly dependendent on the manufacturer and the model of the scanner. To provide a uniform value across different systems, we encoded K in terms of 3 values: 0 (soft reconstruction kernel), 1 (standard reconstruction kernel), and 2 (sharp reconstruction kernel).

To apply a CT acquisition parameter as an external feature, its value is provided as an additional feature in the feature vector of a lesion candidate (Fig. 2). It should be noted that all lesion candidates that are detected within the same CTC scan volume have the same value of a CT acquisition parameter feature. In this study, the external feature was combined with our usual set of conventional image-based shape and texture features (F6; see Section 2.1) of the lesion candidates to construct a vector of 7 features that is analyzed by the classifier of the CAD scheme to reduce FP detections and to determine the final output of the CAD scheme.

2.3 Materials

The training data included the CTC data of 886 patients from 17 institutions. The patients were prepared with cathartic bowel preparation. Orally administered positive-contrast tagging was used with 56 patients. The CTC acquisition was performed in supine and prone positions. There were 158 colonoscopy-confirmed carcinomas or adenomas (called hereafter as "advanced lesions") in 112 patients: 56 were $\geq$10 mm and 102 were 6 – 9 mm in size.

The testing data included the CTC data of 705 patients from 13 institutions. The patients and institutions of the testing data were completely indepdependent from those of the training data. The patients were prepared with cathartic bowel preparation. One third of the patients were administered positive-contrast tagging orally based on iodine alone or with barium. The CTC was performed in supine and prone positions. There were 260 colonoscopy-confirmed advanced lesions in 197 of the 705 patients: 158 of the lesions were $\geq$10 mm and 102 were 6 – 9 mm in size.

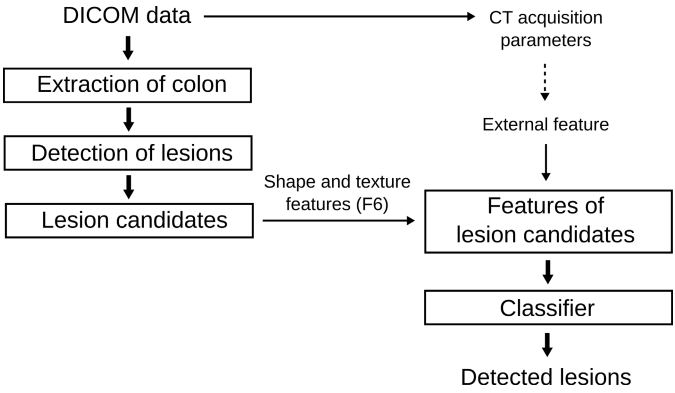

Fig. 2. Application of the CT acquisition parameters as external features within the CAD scheme. Each external feature was combined with the same 6 conventional image-based shape and texture features. A statistical classifier analyzes the features to reduce FP detections.

Table 1 summarizes the value range of the CT acquisition parameters between the training and testing cases.

Table 1. Minimum and maximum values of the CT acquisition parameters in the training and testing cases

	Training		Testing	
Feature	Min.	Max.	Min.	Max.
ST	1.0	5.0	1.0	5.0
RI	1.0	5.0	0.59	2.0
TC	50	408	28	300
RS	0.50	0.97	0.51	0.97
FS	0.7	1.2	0.7	1.2
ET	27	3100	478	1825
K	0	1	0	1
SR	0.10	0.72	0.14	0.79

2.4 Evaluation

To provide clinically meaningful results, we limited the number of detections that can be displayed by the CAD scheme to a maximum of 15 per patient. It is likely that a display of a larger amount of CAD detections, most of which are FP detections, would make the use of computer-assisted interpretation too tedious for clinical practice. Given this constraint, we determined the maximum detection sensitivity and the median number of FP detections per patient.

To assess the statistical significance of the effect of a feature combination on detection accuracy, a pair-wise randomization test was performed by comparing the detection accuracies of CAD using the conventional 6 features (F6) with that of using the F6 together with one of the CT acquisition parameter features. The figure-of-merit (FOM) was the partial area under the free-response receiver-operating characteristic (FROC) curve, where the partial area was calculated to the left from the point where either CAD scheme reached its maximum sensitivity [2].

3 Results

Table 2 shows the per-lesion detection accuracy of CAD in the testing set for all advanced lesions ≥6 mm. The first row (F6) shows the result with the 6 conventional features, whereas the other rows show the result of an indicated combination of 7 features. The use of the SR-feature yielded highest increment in detection sensitivity, but the improvement was not statistically significant.

Table 2. Per-lesion detection accuracy of CAD for advanced polyps and flat lesions. Arrows indicate improvement of detection sensitivity as compared with the original feature set (F6; first row).

Features	Sensitivity ≥10 mm	FPs/case median	Sensitivity 6 – 9 mm	FPs/case median
F6	91%	11	81%	12
F6 + SR	↑92%	15	↑85%	15
F6 + TC	91%	14	77%	15
F6 + ST	↑92%	13	↑84%	12
F6 + RI	↑92%	12	79%	↓9
F6 + K	↑92%	11	↑83%	↓11
F6 + FS	↑92%	↓10	81%	↓10
F6 + RS	91%	12	80%	12
F6 + ET	↑92%	↓10	80%	13

For polyps ≥6 mm, the small improvement in detection accuracy by use of the SR, from 0.71 [0.706, 0.714] to 0.71 [0.710, 0.717] (the numbers in brackets indicate 95% confidence intervals), was not statistically significant. However, for flat lesions ≥6 mm, the use of SR improved the overall per-lesion detection accuracy significantly from 0.68 [0.674, 0.690] to 0.70 [0.689, 0.702] ($p < 0.05$).

Table 3 shows the detection result for advanced flat lesions. Again, the use of the SR yielded most improvement in detection sensitivity. For flat lesions 6 – 9 mm, the improvement in overall detection accuracy from 0.61 $[0.595, 0.624]$ to 0.64 $[0.628, 0.654]$ was statistically significant ($p < 0.01$).

Table 3. Per-lesion detection accuracy for advanced flat lesions. Arrows indicate improvement of detection performance as compared with the original feature set (F6; first row).

Features	Sensitivity ≥10 mm	FPs/case median	Sensitivity 6 – 9 mm	FPs/case median
F6	100%	6	75%	5
F6 + SR	100%	↓4	↑81%	7
F6 + CR	100%	6	63%	14
F6 + ST	100%	↓4	75%	6
F6 + RI	100%	↓4	75%	7
F6 + K	100%	10	75%	11
F6 + FS	100%	8	75%	6
F6 + RS	100%	↓4	75%	8
F6 + ET	100%	8	75%	7

The improvement of overall per-lesion detection accuracy by the SR-feature was highly significant for carcinomas ≥6 mm. The detection accuracy improved from 0.77 $[0.759, 0.773]$ to 0.83 $[0.827, 0.837]$ ($p < 0.000001$). In contrast, for adenomas, the overall per-lesion detection accuracy was reduced marginally but significantly, from 0.77 $[0.771, 0.777]$ to 0.77 $[0.762, 0.768]$ ($p < 0.001$).

4 Discussion

The results indicate that the acquisition parameters of CTC scans can indeed be used successfully as external features to improve the detection accuracy of CAD. However, only few parameters yielded a meaningful improvement, and the precise effect depends on the type of target lesion. In particular, only the SR-feature yielded statistically significant improvements. With SR, the detection accuracy improved significantly in the detection of flat lesions ≥6 mm in size, advanced flat lesions 6 – 9 mm in size, and carcinomas ≥6 mm in size.

It is not particularly surprising that the use of the SR-feature yielded meaningful improvement in CAD performance. In previous studies, CAD performance has been found to be highly dependent on z-axis spatial resolution. The SR features appears to provide meaningful adjunct information about the anisotropy of physical image resolution, thereby improving CAD performance [4].

We used CT acquisition parameters that can be acquired from the header data of DICOM files. A limitation of this approach is the confusion and inconsistency of the terminology that is used by the different manufacturers and their scanner models. For example, some operating modes of the scanners can yield different effective values than what is specified by the DICOM header, and a parameter value may have different effects on different scanners. Therefore, for a practical application, a more detailed scanner-specific analysis of the optimal parameter values may be needed.

Another limitation of the study is that we did not consider combinations of CT acquisition parameter features but we analyzed the effect of each feature one at a time. In combination, they could have a greater impact on improving the detection accuracy of CAD.

5 Conclusion

We investigated the application of CT acquisition parameters as external features with conventional image-based features for improving the detection accuracy of CAD in CTC. A CAD scheme was trained and tested with large independent sets of clinical CTC cases from multiple institutions. The results indicate that the use of the so-called slice-ratio feature in particular can yield significant improvement in the detection of flat lesions and carcinomas.

Acknowledgements. This work was supported in part by grants of Prevent Cancer Foundation, NIH R21CA140934, CA095279, CA166816, and CA131718. We thank Dr. Richard Choi (Virtual Colonoscopy Center, Walter Reed Army Medical Center, Washington, DC, USA) for providing CTC cases for this study. We also thank Partners Research Computing for providing high-performance computing services.

References

1. Bushberg, J., Seibert, J., Leidholdt Jr., E., Boone, J.: The essential physics of medical imaging, 2nd edn. Lippincott Williams & Wilkins, Philadephia (2002)
2. Chakraborty, D.: Analysis of location specific observer performance data: validated extension of the jackknife free-response (JAFROC) method. Acad. Radiol. 13, 1187–1193 (2006)
3. Chowdhury, T., Whelan, P., Ghita, O., Sezille, N., Foley, S.: Development of a synthetic phantom for the selection of optimal scanning parameters in CAD-CT colonography. Med. Eng. Phys. 29, 858–867 (2007)
4. Kim, S., Lee, J., Shin, C., Kim, H., Lee, J., et al.: Effects of spatial resolution and tube current on computer-aided detection of polyps on CT colonographic images: phantom study. Radiology 248, 492–503 (2008)
5. Näppi, J., Yoshida, H.: Automated detection of polyps in CT colonography: evaluation of volumetric features for reduction of false positives. Acad. Radiol. 9, 386–397 (2002)

6. Näppi, J., Yoshida, H.: Feature-guided analysis for reduction of false positives in CAD of polyps for CT colonography. Med. Phys. 30, 1592–1601 (2003)
7. Näppi, J., Yoshida, H.: Fully automated three-dimensional detection of polyps in fecal-tagging CT colonography. Acad. Radiol. 25, 287–300 (2007)
8. Näppi, J., Yoshida, H.: Adaptive correction of the pseudo-enhancement of CT attenuation for fecal-tagging CT colonography. Med. Image Anal. 12, 413–426 (2008)
9. Prokop, M., Galanski, M.: Spiral and multislice computed tomography of the body. Thieme Verlag, Ludwigsburg (2003)
10. Sundaram, P., Beaulieu, C., Paik, D., Schraedley-Desmond, P., Napel, S.: CT colonography: does improved z resolution help computer-aided polyp detection? Med. Phys. 30, 2663–2674 (2003)
11. Yoshida, H., Näppi, J.: Three-dimensional computer-aided diagnosis scheme for detection of colonic polyps. IEEE Trans. Med. Imaging 20, 1261–1274 (2001)
12. Yoshida, H., Näppi, J., MacEneaney, P., Rubin, D., Dachman, A.: Computer-aided diagnosis scheme for detection of polyps at CT colonography. Radiographics 22, 963–979 (2002)